Proc. 8th Int. Conf. Quarks and Nuclear Physics (QNP2018)
JPS Conf. Proc. **26**, 011004 (2019)
https://doi.org/10.7566/JPSCP.26.011004

Baryon Interactions from Lattice QCD

Tetsuo Hatsuda
RIKEN Interdisciplinary Theoretical and Mathematical Sciences Program (iTHEMS), 2-1 Hirosawa, Wako, Saitama 351-0198, Japan
E-mail: thatsuda@riken.jp

(Received February 18, 2019)

Two theoretical approaches (the direct method and the HAL QCD method) to study the baryon-baryon interactions in lattice QCD are reviewed with critical comparison between the two. The direct method is shown to have fatal problems in extracting two-baryon ground state energy. We present some applications of the HAL QCD method, which is a useful tool to study multi baryons in a controlled way, to the exotic dibaryons with the Ω-baryon.

KEYWORDS: Lattice QCD, Baryon interaction, Exotic hadron

1. Introduction

Baryon-baryon interactions have been studied by two methods in lattice QCD. The first one is the HAL QCD method [1–4], which derives the energy-independent non-local kernel (non-local potential) from the tempo-spatial correlations of two baryons: The binding energies and phase shifts in the infinite volume are calculated through the Schrödinger-type equation obtained from the reduction formula for composite operators [2]. The second one is the direct method [5, 6], which calculates the binding energies and scattering phase shifts from eigenenergies on the lattice by using the Lüscher's finite volume formula [7, 8]. Both methods rely on the asymptotic behavior of the Nambu-Bethe-Salpeter (NBS) wave function for short-range hadronic interactions.

In a series of our recent papers [9–13], we have carefully examined the systematic uncertainties in both methods. The difficulty of two-baryon systems compared to a single baryon originates from the existence of elastic scattering states. Their typical excitation energies δE are one to two orders of magnitude smaller than $O(\Lambda_{\rm QCD})$, so that one needs to probe large Euclidean time $t \gtrsim (\delta E)^{-1}$ to extract the genuine signal of the ground state (ground state saturation) in the direct method. However, the statistical fluctuation increases exponentially in t as well as the baryon number A for multi-baryon systems as proved in [14, 15]. This practically prevents one to identify the true ground state in the direct method. Indeed, our extensive studies [9, 10] showed that a commonly employed procedure in the direct method to identify plateaux at early time slices, $t \ll (\delta E)^{-1}$, suffers from uncontrolled systematic errors from the excited state contaminations. The typical symptoms of such systematics in previous studies of the direct method were explicitly exposed by the normality check based on the Lüscher's finite volume formula and the analyticity of the S-matrix [10].

On the other hand, the time-dependent HAL QCD method [3] is free from the problem of ground state saturation, since the energy-independent potential is extracted from the spatial and temporal correlations with the information of both the ground and excited states associated with the elastic scattering. In practical calculations, the derivative expansion of the potential is found to have good convergence at low energies. Also, contaminations from the inelastic states and the effect of the finite volume have been shown to be well under control (see [12] and references therein.)

In the present article, we highlight the problems of the direct method on the basis of Ref. [13]. Then, we show two successful examples of the HAL QCD method; the ΩΩ and $N\Omega$ interactions.

2. The direct method

In the direct method for two-baryon systems, the energy eigenvalues on a finite volume are measured by the temporal correlation of the two-baryon operator, $\mathcal{J}_{BB}^{\rm sink,src}(t)$;

$$C_{\rm BB}(t) \equiv \langle 0|\mathcal{J}_{BB}^{\rm sink}(t)\overline{\mathcal{J}}_{BB}^{\rm src}(0)|0\rangle = \sum_n Z_n e^{-W_n t} + \cdots , \tag{1}$$

where W_n is the energy of n-th two-baryon elastic state and the ellipsis denotes the inelastic contributions. In order to obtain the energy shifts $\Delta E_n \equiv W_n - 2m_B$ with m_B being the single baryon mass, one often uses the ratio of the temporal correlation function of two- (one-) baryon system $C_{\rm BB}(t)$ ($C_{\rm B}(t)$) as $R(t) \equiv C_{\rm BB}(t)/\{C_{\rm B}(t)\}^2, C_B(t) = Z_B e^{-m_B t} + \cdots$. The energy shift of the ground state can be obtained from the plateau value of the effective energy shift defined by

$$\Delta E_{\rm eff}(t) \equiv \frac{1}{a}\log\left(\frac{R(t)}{R(t+a)}\right), \tag{2}$$

with a being the lattice spacing. Here t needs to be sufficiently larger than the inverse of the excitation energy to achieve the ground state saturation. Once the energy shift of the ground state on a finite volume is obtained reliably, one may calculate the scattering phase shift in the infinite volume, $\delta_0(k)$, via the Lüscher's finite volume formula [8],

$$k\cot\delta_0(k) = \frac{1}{\pi(La)}\sum_{\vec{n}\in\mathbf{Z}^3}\frac{1}{\vec{n}^2 - q^2}, \qquad q = \frac{k(La)}{2\pi}, \tag{3}$$

where we consider the S-wave scattering for simplicity, k is defined through $W_n = 2\sqrt{m_B^2 + k^2}$ and L is the number of the spatial sites of the lattice box.

As noted in the Introduction, the origin of the difficulty of two-baryon systems is the existence of elastic scattering states. Since the typical excitation energy of such states is $(2\pi)^2/((La)^2 m_B)$, the ground state saturation requires extremely large t, e.g., $t \gtrsim O(10)$ fm at $La = 8$ fm and $m_B = 1$ GeV. Then the bad signal-to-noise ratio for such large t makes it practically impossible to obtain signals. However, in the literature of the direct method [5, 6], extraction of the energy shift for the ground state is attempted at early time slices as small as $t \sim O(1)$ fm. Such a procedure has no theoretical justification and can indeed be shown to fail [9–13].

3. Normality check of the direct method

A "normality check" on the direct method on the basis of the Lüscher's finite volume formula and the analyticity of the S-matrix was introduced in Ref. [10]. Two examples of the normality check are given in Fig. 1, where $k\cot\delta_0(k)$ is plotted as a function of k^2 for $NN(^1{\rm S}_0)$. Red and blue lines in Fig. 1 represent fits to data by the effective range expansion (ERE) at the next-to-leading order (NLO) as

$$k\cot\delta_0(k) \quad \simeq \quad \frac{1}{a_0} + \frac{r_0}{2}k^2, \tag{4}$$

where a_0 and r_0 are the scattering length and the effective range, respectively. In Fig. 1 (Left), inconsistency in ERE parameters is observed: The NLO ERE fit obtained from the data at $k^2 < 0$ on finite volumes (red line) disagrees with the fit to the data at $k^2 > 0$ on finite volumes together with the infinite volume limit at $k^2 < 0$ (blue line). For the latter fit (the blue line), the physical condition of the bound state pole is also violated. In Fig. 1 (Right), the NLO ERE fit exhibits a singular behavior as the divergent effective range. These indicate that the plateau fitting at $t \simeq 1$ fm suffers from large uncontrolled systematic errors probably due to contaminations from the excited states.

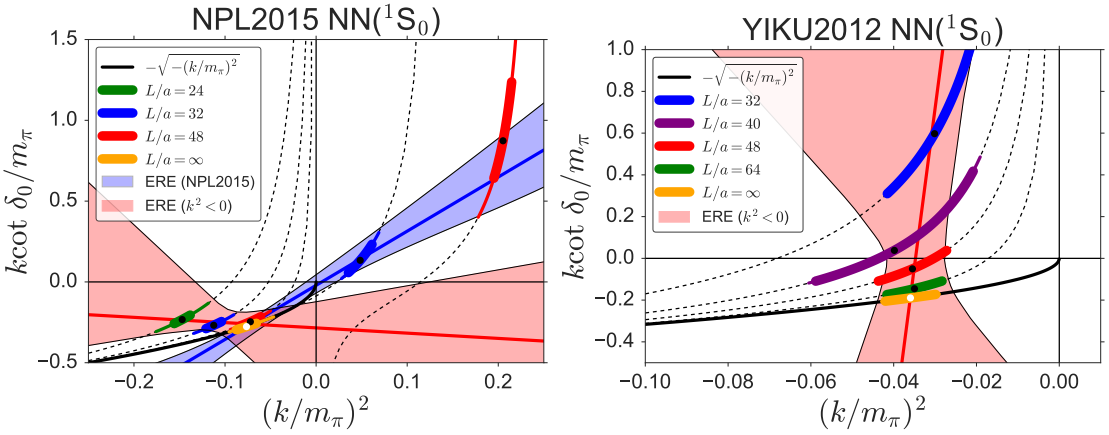

Fig. 1. $k\cot\delta_0(k)/m_\pi$ as a function of $(k/m_\pi)^2$ for $NN(^1\mathrm{S}_0)$ on each volume and the infinite volume in the direct method from Ref. [17] (Left) and Ref. [18] (Right). Black dashed lines correspond to the Lüscher's formula for each volume, while the black solid line represents the bound-state condition, $-\sqrt{-(k/m_\pi)^2}$. The red line (with an error band) corresponds to the ERE obtained from the data at $k^2 < 0$ on finite volumes. In the left figure, the ERE fit to the data at $k^2 > 0$ on finite volumes together with only the infinite volume limit at $k^2 < 0$ is also shown by the blue line. Both figures are taken from Ref. [10].

4. The HAL QCD method

In the time-dependent HAL QCD method, one starts from the four-point correlation function of the two-baryon system $F(\vec{r},t)$;

$$F(\vec{r},t) \equiv \langle 0|T\{\sum_{\vec{x}} B(\vec{x}+\vec{r},t)B(\vec{x},t)\overline{\mathcal{J}}^{\mathrm{src}}_{BB}(0)\}|0\rangle = \sum_n A_n \psi^{W_n}(\vec{r})e^{-W_n t} + \cdots, \tag{5}$$

where $A_n \equiv \langle 2B, W_n|\overline{\mathcal{J}}^{\mathrm{src}}_{BB}(0)|0\rangle$ is the overlap factor and the ellipsis represents the inelastic contributions. The so-called "$\mathcal{R}$-correlator" is defined as

$$\mathcal{R}(\vec{r},t) \equiv \frac{F(\vec{r},t)}{\{C_B(t)\}^2} = \sum_n \frac{A_n}{Z_B^2}\psi^{W_n}(\vec{r})e^{-(W_n-2m_B)t} + \cdots. \tag{6}$$

The elastic part of $\mathcal{R}(\vec{r},t)$ satisfies an integro-differential equation [3,4],

$$\left[-H_0 - \frac{\partial}{\partial t} + \frac{1}{4m_B}\frac{\partial^2}{\partial t^2}\right]\mathcal{R}(\vec{r},t) = \int d\vec{r}' U(\vec{r},\vec{r}')\mathcal{R}(\vec{r}',t). \tag{7}$$

Below the inelastic threshold W_{th}, the potential $U(\vec{r},\vec{r}')$ is shown to be faithful to the phase shifts, which are encoded in the behavior of the NBS wave function at large r. Eq. (7) requires neither the ground state saturation nor the determination of individual eigenenergy W_n. Therefore, in contrast to the direct method, the condition required for the reliable calculation is much more relaxed in the time-dependent HAL QCD method as $t \gtrsim O(\Lambda_{\mathrm{QCD}}^{-1}) \sim O(1)$ fm.

In practice, we expand the non-local potential as

$$U(\vec{r},\vec{r}') = \sum_n V_n(\vec{r})\nabla^n\delta(\vec{r}-\vec{r}'). \tag{8}$$

For the spin-singlet channel, the leading-order (LO) truncation of the expansion reads $U(\vec{r},\vec{r}') \simeq V_0^{\mathrm{LO}}(\vec{r})\delta(\vec{r}-\vec{r}')$, while the next-to-next-leading order (N^{2}LO) truncation reads $U(\vec{r},\vec{r}') \simeq \{V_0^{\mathrm{N^2LO}}(\vec{r}) + V_2^{\mathrm{N^2LO}}(\vec{r})\nabla^2\}\delta(\vec{r}-\vec{r}')$.

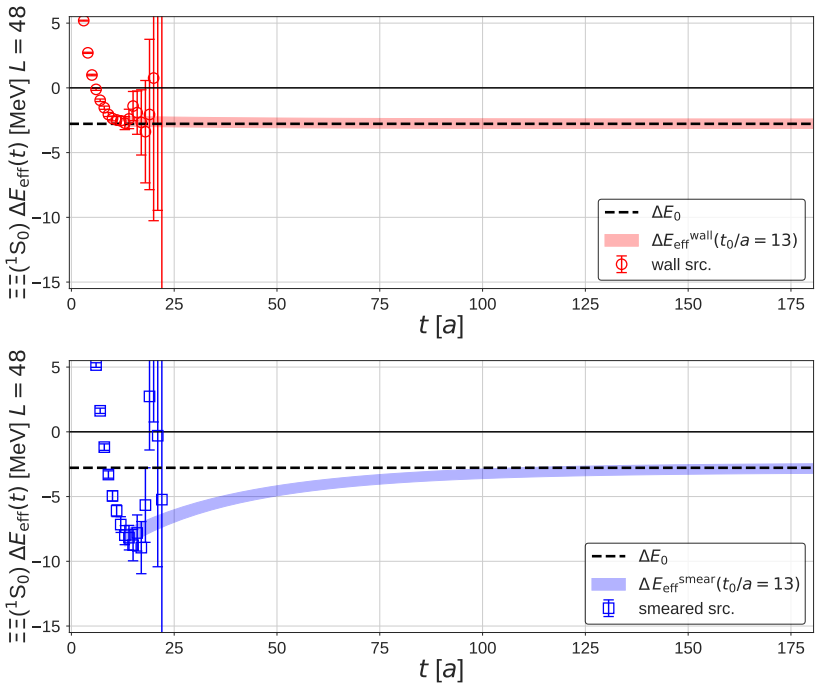

Fig. 2. The effective energy shifts for the wider range of the Euclidean time t. This figure is taken from [13].

5. Large t behavior of the effective energy shifts

Once the potential in (8) is obtained, one can construct an effective Hamiltonian (HAL QCD Hamiltonian $H^{\rm HAL}$) which can be solved either in the finite volume or in the infinite volume, so that one can obtain the wave functions and eigenenergies of the the ground state and excited states in the elastic channel. Then, one can explicitly check how much excited state contamination presents in the effective energy shift [13].

To illustrate the effect of the excited state contamination, we consider S-wave $\Xi\Xi$ interaction in the spin-singlet channel. We denote the energy shift of the n-th eigenstate obtained by the HAL QCD Hamiltonian $H^{\rm HAL}$ as ΔE_n. Then the temporal correlation $R(t)$ measured on the lattice is approximated, for sufficiently large t where the inelastic contribution can be neglected, by the "reconstructed" correlation $R_{\rm rc}$, as $R(t) \simeq R_{\rm rc}(t, t_0) = \sum_{n=0}^{n_{\rm max}} b_n(t_0) e^{-\Delta E_n t}$. Here $n_{\rm max}$ is the number of elastic states below the inelastic threshold (e.g. $n_{\rm max} = 3, 4, 6$ for $L = 40, 48, 64$, respectively, in the present case), while t_0 is a Euclidean time at which the coupling of the source operator to each state $b_n(t_0)$ is determined. Then we can define the effective energy-shift in which the excited state contamination is taken into account [13];

$$\Delta E_{\rm eff}(t, t_0) \equiv \frac{1}{a} \log\left(\frac{R_{\rm rc}(t, t_0)}{R_{\rm rc}(t + a, t_0)}\right). \tag{9}$$

For the baryon source operator, we use two different quark sources with the Coulomb gauge fixing, the wall source, $q^{\rm wall}(t) = \sum_{\vec{y}} q(\vec{y}, t)$ with $q(\vec{y}, t)$ being the quark operator, mainly used in the HAL QCD method, and the smeared source, $q^{\rm smear}(\vec{x}, t) = \sum_{\vec{y}} f(|\vec{x} - \vec{y}|) q(\vec{y}, t)$, often used in the direct method. For the smearing function, we take $f(r) \equiv \{Ae^{-Br}, 1, 0\}$ for $\{0 < r < (L-1)/2,\ r = 0,\ (L-1)/2 \le r\}$, respectively, as in Ref. [18], and the center of the smeared source is same for all six quarks (i.e., zero displacement between two baryons), as has been employed in all previous studies in the direct method. For both sources, we consider the point-sink operator for each baryon.

Numerical data are taken from the (2+1)-flavor lattice QCD ensembles generated in Ref. [18] with the Iwasaki gauge action and nonperturbatively $O(a)$-improved Wilson quark action at the lattice spacing $a = 0.08995(40)$ fm ($a^{-1} = 2.194(10)$ GeV). Up and down quark masses are chosen to be relatively heavy, while strange quark mass is physical, so that the light hadron masses are $m_\pi = 0.51$ GeV, $m_K = 0.62$ GeV, $m_N = 1.32$ GeV and $m_\Xi = 1.46$ GeV.

In Fig. 2, the raw numerical data of $\Delta E_{\rm eff}(t)$ for $L = 48$ are shown for two source operators together with the corresponding values of ΔE_0 and $\Delta E_{\rm eff}(t, t_0)$ (with t_0/a=13). First of all, the explosion of statistical error bars already takes place below $t/a = 25$. Secondly, pseudo-plateaux appear around $t/a = 15$ in both wall and smeared sources, but the effective energy shift are different by factor 2. These two points imply that one cannot conclude anything about the ground state energy from the short-time behavior of the effective energy shift.

Now, the dashed lines (ΔE_0) and the red/blue band ($\Delta E_{\rm eff}(t, t_0)$) in the figures are the prediction on the behavior of the effective energy shift obtained from the HAL QCD Hamiltonian with exactly the same gauge configurations. One finds that the approach to the ground state saturation is quite different between the two sources. Also, the predicted $\Delta E_{\rm eff}(t, t_0)$ can reproduce the raw data nicely in the early-time region. In the previous works in the direct method [5, 6], the smeared source with all 6-quark are localized on top of each other is exclusively used for two baryons under the bold assumption that it couples to the two-baryon ground state dominantly. The lower panel of Fig. 2 shows explicitly that such an assumption has no ground. To get the real ground state saturation for the present smeared source, the true value of ΔE_0 is obtained only for $t/a \sim 100$ which is not attainable due to exponentially increasing statistical errors for large t. The HAL QCD method, which utilizes not only the temporal correlation but also the spatial correlation, is free from such problem to obtain ΔE_0.

6. ΩΩ and $N\Omega$ Interactions

As is clear from the discussions in previous sections, baryon-baryon interaction can be studied reliably in the HAL QCD method but not in the direct method. Let us now consider rather exotic two-baryon systems with Ω-baryon. Since Ω is stable under strong interaction, there is a possibility to have new quasi-stable dibaryons, such as ΩΩ [20] and $N\Omega$ [21]. For other baryon-baryon interactions with the HAL QCD method, see [19].

To make our calculations realistic, we take the gauge configurations at nearly physical quark masses ($m_\pi \simeq 146$ MeV and $m_K \simeq 525$ MeV) generated by using the (2+1)-flavor lattice QCD

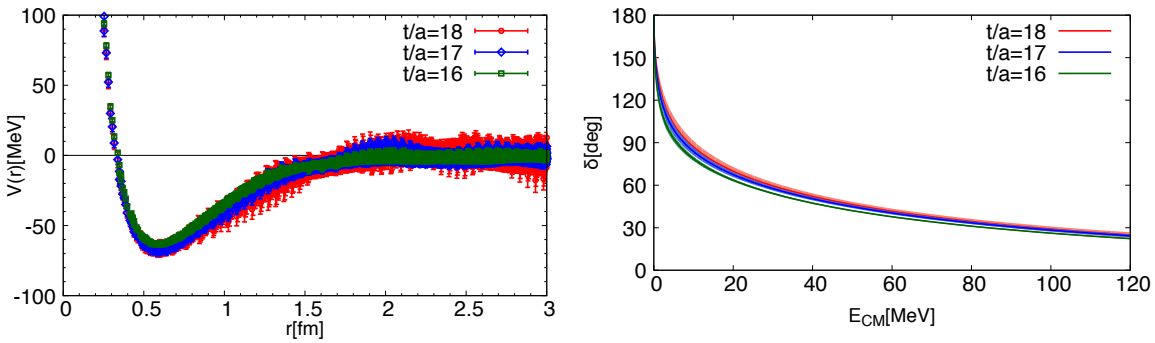

Fig. 3. (Left) The ΩΩ potential $V(r)$ in the $^1S_0$ channel at Euclidean time $t/a = 16, 17$, and 18. (Right) The ΩΩ phase shift $\delta(k)$ in the $^1S_0$ channel for $t/a = 16, 17$ and 18 as a function of the center of mass kinetic energy $E_{\rm CM} = 2\sqrt{k^2 + m_\Omega^2} - 2m_\Omega$.

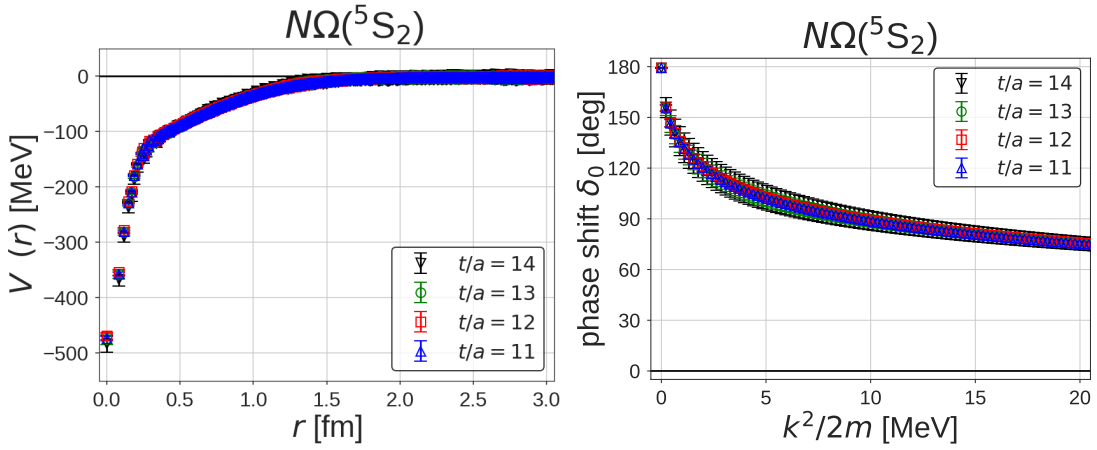

Fig. 4. (Left) The central potential $V(r)$ of the $N\Omega(^5S_2)$ system at $t/a = 11$ (blue up-pointing triangles), 12 (red squares), 13 (green circles) and 14 (black down-pointing triangles). (Right) The S-wave scattering phase shifts δ_0 as a function of the center of mass kinetic energy, $k^2/2m$, with m being the reduced mass of N and Ω.

with the Iwasaki gauge action at $\beta = 1.82$ and the non-perturbatively $O(a)$-improved Wilson quark action. The lattice cutoff is $a^{-1} \simeq 2.333$ GeV ($a \simeq 0.0846$ fm) and the lattice volume L^4 is 96^4, corresponding to $La \simeq 8.1$ fm [22]. We employ the wall-type quark source with the Coulomb gauge fixing. The periodic (Dirichlet) boundary condition for the spatial (temporal) direction is imposed for quarks. The fit to the effective mass in the range $12 \le t/a \le 17$ for N and $17 \le t/a \le 22$ for Ω lead to $m_N = 954.7(2.7)$ MeV and $m_\Omega = 1711.5(1.0)$ MeV. These values are about 2% heavier than physical values due to a slight difference of the present quark masses from the physical point.

Shown in Fig. 3 (Left) is the $^1S_0$ potential $V_0^{\rm LO}(r)$ for $t/a = 16, 17$, and 18. The particular region $t/a = 17 \pm 1$ in Fig. 3 is chosen to suppress contamination from excited states in the single Ω propagator at smaller t and simultaneously to avoid large statistical errors at larger t. We observe that the potentials at $t/a = 16, 17$, and 18 are nearly identical within statistical errors. The $\Omega\Omega$ potential $V(r)$ has qualitative features similar to the central potential of the nucleon-nucleon (NN) interaction, i.e., the short range repulsion and the intermediate range attraction. There are, however, two quantitative differences: (i) the short range repulsion is much weaker in the $\Omega\Omega$ case possibly due to the absence of quark Pauli exclusion effect, and (ii) the attractive part is much short-ranged possibly due to the η exchange instead of the pion exchange. The $\Omega\Omega$ scattering phase shift $\delta(k)$ in the $^1S_0$ channel obtained from $V_{\rm fit}(r)$ (fit of $V(r)$ by a combination of analytic functions) is shown in Fig. 3 (Right) for $t/a = 16, 17$, and 18 as a function of the kinetic energy in the center of mass frame, $E_{\rm CM} = 2\sqrt{k^2 + m_\Omega^2} - 2m_\Omega$. The error bands reflect the statistical uncertainty of the potential in Fig. 3 (Left). All three cases show that $\delta(0)$ starts from 180°, which indicates the existence of a bound $\Omega\Omega$ system.

Shown in Fig. 4 (Left) is the $^1S_0$ potential $V_0^{\rm LO}(r)$ for $t/a = 11-14$. These potentials are consistent with each other within statistical errors, which is an indirect evidence of the small coupling with the D-wave octet-octet states below the $N\Omega$ threshold in the spin-2 channel as suggested in [23]. (Such a stability of the potential in the same range of t is not found for the spin-1 $N\Omega$ system which can couple to the S-wave octet-octet states below threshold.) Shown in Fig. 4 (Right) is the S-wave scattering phase shift δ_0 as a function of the kinetic energy. In the $k \to 0$ limit, the phase shift approaches to 180°. This implies that the existence of a quasi-bound state of $N\Omega$ in the $^5S_2$ channel.

In Fig. 5, we summarize the binding energies and the root mean square distances of the possible qusi-stable dibaryons, $\Omega\Omega$ (diOmega) and $N\Omega$ together with the deuteron (the only known dibaryon so far). Coulomb interactions are taken into account. The error bars are obtained by the quadrature

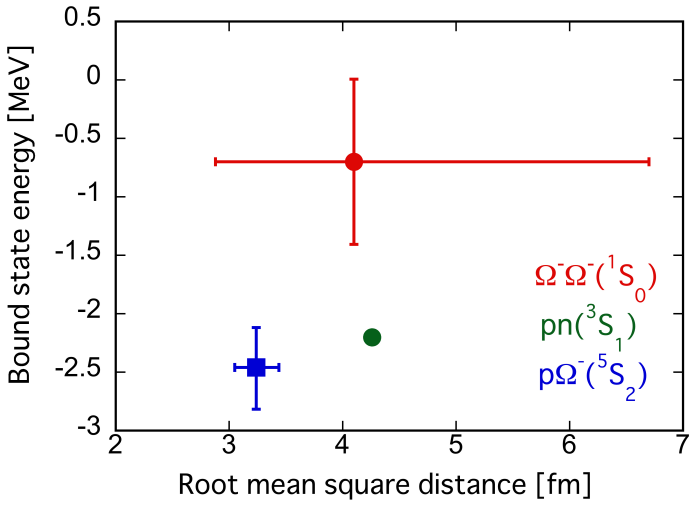

Fig. 5. The binding energy vs. the root mean square distance for strange dibaryon candidates as well as the experimental data for the deuteron.

of the statistical and systematic errors. The figure shows that they are all loosely bound systems with small binding energies and large radii. From the experimental point of view, the femtoscopy analysis in pp, pA and AA collisions at RHIC and LHC would be one of the promising ways to study such exotic dibaryons [24–26].

7. Summary

In the present article, we summarized the problems of studying the temporal (t) correlation functions for multi-baryon systems: Exponentially increasing statistical noise for large t and the effect of the elastic scattering states with small gaps for large volume (L^3) prevent one to extract information of the ground state in the direct method. On the other hand, the HAL QCD method, which combines the temporal and spatial correlation functions of two baryons, turns out to be useful to extract the baryon-baryon phase shifts and binding energies in a controlled manner. We showed some applications of the HAL QCD method to exotic dibaryons, $\Omega\Omega$ (diOmega) and $N\Omega$, with the (2+1)-flavor lattice QCD simulations at nearly physical quark masses. They are found to be possible quasi-stable dibaryons, and could be studied experimentally by two-baryon momentum correlations at RHIC and LHC.

Acknowledgement

The author thanks the members of the HAL QCD Collaboration, in particular, Takumi Iritani who made a major contribution to the topics covered in the present article. This work was partially supported by RIKEN iTHEMS program and by the JSPS grant No.18H05236.

References

[1] N. Ishii, S. Aoki and T. Hatsuda, Phys. Rev. Lett. **99**, 022001 (2007) [arXiv:nucl-th/0611096].
[2] S. Aoki, T. Hatsuda and N. Ishii, Prog. Theor. Phys. **123**, 89 (2010) [arXiv:0909.5585 [hep-lat]].
[3] N. Ishii *et al.* [HAL QCD Collaboration], Phys. Lett. **B712**, 437 (2012) [arXiv:1203.3642 [hep-lat]].
[4] S. Aoki *et al.* [HAL QCD Collaboration], Prog. Theor. Exp. Phys. **2012**, 01A105 (2012) [arXiv:1206.5088 [hep-lat]].
[5] T. Yamazaki, K. i. Ishikawa, Y. Kuramashi and A. Ukawa, Phys. Rev. D **92**, 014501 (2015) [arXiv:1502.04182 [hep-lat]], and references therein.
[6] M. L. Wagman, F. Winter, E. Chang, Z. Davoudi, W. Detmold, K. Orginos, M. J. Savage and P. E. Shanahan, Phys. Rev. D **96**, 114510 (2017) [arXiv:1706.06550 [hep-lat]], and references therein.
[7] M. Lüscher, Commun. Math. Phys. **104**, 177 (1986); *ibid.*, **105**, 153 (1986).
[8] M. Lüscher, Nucl. Phys. B **354**, 531 (1991).
[9] T. Iritani *et al.* [HAL QCD Collaboration], JHEP **1610**, 101 (2016) [arXiv:1607.06371 [hep-lat]].
[10] T. Iritani *et al.*, Phys. Rev. D **96**, 034521 (2017) [arXiv:1703.07210 [hep-lat]].
[11] S. Aoki, T. Doi and T. Iritani, EPJ Web Conf. **175**, 05006 (2018) [arXiv:1707.08800 [hep-lat]].
[12] T. Iritani *et al.* [HAL QCD Collaboration], Phys. Rev. D **99**, 014514 (2019) [arXiv:1805.02365 [hep-lat]].
[13] T. Iritani *et al.* [HAL QCD Collaboration], JHEP **1903**, 007 (2019) [arXiv:1812.08539 [hep-lat]].
[14] G. Parisi, Phys. Rept. **103**, 203 (1984).
[15] G. P. Lepage, CLNS-89-971, in *From Actions to Answers: Proceedings of the TASI 1989*, edited by T. Degrand and D. Toussaint (World Scientific, Singapore, 1990).
[16] K. Murano, N. Ishii, S. Aoki and T. Hatsuda, Prog. Theor. Phys. **125**, 1225 (2011) [arXiv:1103.0619 [hep-lat]].
[17] K. Orginos, A. Parreno, M. J. Savage, S. R. Beane, E. Chang and W. Detmold, Phys. Rev. D **92**, 114512 (2015) [arXiv:1508.07583 [hep-lat]].
[18] T. Yamazaki, K. i. Ishikawa, Y. Kuramashi and A. Ukawa, Phys. Rev. D **86**, 074514 (2012) [arXiv:1207.4277 [hep-lat]].
[19] T. Inoue [HAL QCD Collaboration], arXiv:1809.08932 [hep-lat].
[20] S. Gongyo *et al.* [HAL QCD Collaboration], Phys. Rev. Lett. **120**, 212001 (2018) [arXiv:1709.00654 [hep-lat]].
[21] T. Iritani *et al.* [HAL QCD Collaboration], arXiv:1810.03416 [hep-lat].
[22] K.-I. Ishikawa *et al.* [PACS Coll.], PoS LATTICE **2015**, 075 (2016) [arXiv:1511.09222 [hep-lat]].
[23] T. Sekihara, Y. Kamiya and T. Hyodo, Phys. Rev. C **98**, 015205 (2018) [arXiv:1805.04024 [hep-ph]].
[24] K. Morita, A. Ohnishi, F. Etminan and T. Hatsuda, Phys. Rev. C **94**, 031901 (2016) [arXiv:1605.06765 [hep-ph]].
[25] T. Hatsuda, K. Morita, A. Ohnishi and K. Sasaki, Nucl. Phys. A **967**, 856 (2017) [arXiv:1704.05225 [nucl-th]].
[26] V. Mantovani Sarti, in these proceedings.